


Expression and Cellular Distribution of P-Glycoprotein and Breast Cancer Resistance Protein in Amyotrophic Lateral Sclerosis Patients

Erwin A. van Vliet , PhD, Anand M. Iyer, PhD, Lucia Mesarsova, PhD, Hilal Çolakoglu, BSc, Jasper J. Anink, BSc, Olaf van Tellingen, PhD, Nicholas J. Maragakis, MD, PhD, Jeremy Shefner, MD, PhD, Ton Bunt, MD, MBA, and Eleonora Aronica, MD, PhD

Abstract

For amyotrophic lateral sclerosis (ALS), achieving and maintaining effective drug levels in the brain is challenging due to the activity of ATP-binding cassette (ABC) transporters which efflux drugs that affect drug exposure and response in the brain. We investigated the expression and cellular distribution of the ABC transporters P-glycoprotein (P-gp) and breast cancer resistance protein (BCRP) using immunohistochemistry in spinal cord (SC), motor cortex, and cerebellum from a large cohort of genetically well characterized ALS patients (n = 25) and controls (n = 14). The ALS group included 17 sporadic (sALS) and 8 familial (fALS) patients. Strong P-gp expression was observed in endothelial cells in both control and ALS specimens. Immunohistochemical analysis showed higher P-gp expression in reactive astroglial cells in both gray (ventral horn) and white matter of the SC, as well as in the motor cortex of all ALS patients, as compared with controls. BCRP expression was higher in glia in the SC and in blood vessels and glia in the motor cortex of ALS patients, as compared with controls. P-gp and BCRP immunoreactivity did not differ between sALS and fALS cases. The upregulation of both ABC transporters in the brain may explain multidrug

resistance in ALS patients and has implications for the use of both approved and experimental therapeutics.

Key Words: Amyotrophic lateral sclerosis (ALS), Astrocytes, BCRP, Blood vessels, Motor cortex, Multidrug resistance, P-glycoprotein (P-gp), Spinal cord.

INTRODUCTION

Amyotrophic lateral sclerosis (ALS) is a progressive and fatal neurodegenerative disorder that primarily affects motor neurons in the cerebral cortex, brainstem, and spinal cord (SC). Mounting evidence suggests that it is a complex multi-system neurodegenerative disorder with considerable phenotypic heterogeneity and widespread central nervous system (CNS) involvement (1–3). Approximately 90% of ALS cases arise spontaneously, while the remaining 10% show predominantly autosomal dominant inheritance. Since the discovery of mutations in the $\text{Cu}^{2+}/\text{Zn}^{2+}$ superoxide dismutase (SOD1) gene and the C9orf72 mutation (each of which is responsible for 20% and 30%, respectively, of the familial ALS cases [4, 5]), a broad range of both causative and disease modifying gene variants have been associated with both sporadic and familial forms of ALS (reviewed in [3, 6]). This wide range of genetic influences reflects the complexity of the disease involving heterogeneous converging mechanisms, including RNA processing and stability, proteostasis impairment, mitochondrial dysfunction, increased oxidative stress, and neuroinflammation (7–9). Thus, combination therapies targeting more than one disease-related cellular pathway may be required for efficient control of the pathological cascade contributing to motor neuron degeneration (10, 11). An important challenge for new and existing therapies is the need to maintain therapeutic exposure in the brain and SC, which are protected by the blood-brain barrier (BBB). Beyond simply acting as a passive barrier, recent attention has been focused on BBB-driven drug-resistance in ALS, mediated by the ATP-binding cassette (ABC) drug efflux transporters ([12]; for reviews see [13, 14]).

Several studies provide evidence of impairment of blood-brain and blood-spinal cord barrier function at an early

From the Amsterdam UMC, University of Amsterdam, Department of (Neuro)Pathology, Amsterdam Neuroscience (EA vV, AMI, LM, JJA, EA); Swammerdam Institute for Life Sciences, Center for Neuroscience, University of Amsterdam (EA vV); Division of Pharmacology, The Netherlands Cancer Institute (HC, OvT), Amsterdam, The Netherlands; Department of Neurology, The Johns Hopkins University School of Medicine, Baltimore, Maryland (NJM); Department of Neurology, Barrow Neurological Institute, Phoenix, Arizona (JS); and Izumi Biosciences, Inc., Lexington, Massachusetts (TB)

Send correspondence to: Erwin A. van Vliet, PhD, Amsterdam UMC, University of Amsterdam, Academic Medical Center, Department of (Neuro)Pathology, Meibergdreef 9, 1105 AZ Amsterdam, The Netherlands; E-mail: e.a.vanvliet@uva.nl

This study was supported by the Stichting ALS Nederland, “The Dutch ALS Tissue Bank” (A.E.) and the Muscular Dystrophy Association (MDA) Venture Philanthropy grant; T.B.).

T.B. is a chief Executive Officer, founder, and president of Izumi Biosciences and develops oral IZ10023 for patient trials. Together with O.v.T. he applied for a patent (US 20140235631, “Efflux inhibitor compositions and methods of treatment using the same”).

Supplementary Data can be found at academic.oup.com/jnen.

stage in both patients and animal models of ALS (for reviews see [14, 15]). The compensatory overexpression of ABC efflux transporter proteins P-glycoprotein (P-gp)/ABCB1 and breast cancer resistance protein (BCRP)/ABCG2 that protect affected tissues by pumping foreign substances and drugs out is a common feature of diseases associated with multidrug resistance (16–18). Overexpression of P-gp in ALS mutant mice has been demonstrated, suggesting a possible contribution of these pumps toward drug resistance in ALS patients (12, 19–24). As an example of the importance of this mechanism, Jablonski et al showed improved effects of riluzole in SOD1 transgenic mice when administered in combination with the dual P-gp/BCRP inhibitor elacridar (21). The hypothesis that ABC drug efflux transporters may impact CNS distribution of therapeutic agents in ALS patients is supported by the observation that expression of P-gp and BCRP was increased in SC extracts from 3 ALS patients (12). However, the cellular distribution of P-gp and BCRP within the affected human motor cortex and SC was not shown and the cohort studied was very small.

The aim of this study is to investigate the expression patterns of 2 ABC efflux transporters, P-gp and BCRP in SC, motor cortex (MCx), and cerebellum from a large, genetically well-characterized cohort of patients with sporadic or familial forms of ALS.

MATERIALS AND METHODS

Subjects

Postmortem material was obtained at autopsy from 25 ALS patients at the department of (Neuro)pathology of the Amsterdam UMC, Academic Medical Center, University of Amsterdam, the Netherlands. All patients fulfilled the diagnostic criteria for ALS (El Escorial criteria [25]) as reviewed independently by 2 neuropathologists. All patients with ALS died from respiratory failure. Control SC tissue was obtained from 14 patients who had died from a nonneurological disease. ALS and control patients included in the study did not show any sign of infection before death. The ALS patients included in the study did not receive medications such as riluzole or edaravone that are substrates of P-gp and/or BCRP. Informed consent was obtained for the use of brain tissue and for access to medical records for research purposes and approval was obtained from the relevant local ethical committees for medical research. All autopsies were performed within 12 hours after death.

Tissue Preparation

Paraffin-embedded tissue was sectioned at 6 μ m and mounted on precoated glass slides (StarFrost, Waldemar Knittel Glasbearbeitungs GmbH, Braunschweig, Germany). Representative sections of all specimens were processed for hematoxylin and eosin, Klüver-Barrera or Nissl staining. To define different cell populations serial sections were stained with Nissl, astroglial and microglial markers (glial fibrillary acidic protein [GFAP] and HLA-DR, see following paragraph).

Immunohistochemistry

Sections were deparaffinated in xylene, rinsed in ethanol (100%, 96%, 70%) and incubated for 20 minutes in 0.3% hydrogen peroxide diluted in methanol. Antigen retrieval was performed using a pressure cooker in 0.01 M sodium citrate, pH 6.0 at 121°C for 10 minutes. Slides were washed with phosphate-buffered saline (pH 7.4) and incubated overnight with primary antibody. GFAP (polyclonal rabbit, DAKO, Glostrup, Denmark; 1:4000), vimentin (mouse clone V9, DAKO; 1:400), major histocompatibility complex class II antigen (HLA)-DP, DQ, DR (mouse clone CR3/43; DAKO; 1:400), or CD68 (mouse clone PG-M1, DAKO; 1:200) was used in the routine immunohistochemical analysis of ALS specimens. For the detection of P-gp we used a monoclonal mouse antibody (IgG1, JSB-1, 1:40; Abcam, Cambridge, UK) as well as for BCRP (IgG2a, BXP-21, 1:100; Abcam). Single-label immunohistochemistry was performed as previously described (26) with the Brightvision kit (Immunologic, Duiven, the Netherlands) and Bright DAB (Immunologic) as the chromogen.

To determine whether P-gp and BCRP colocalized with endothelial cells and astrocytes, sections were first incubated with respectively CD34 (mouse clone QBEnd10; Immunotech, Marseille, France; 1:600) or GFAP (polyclonal rabbit, DAKO; 1:4000) for 1 hour at room temperature, followed by staining using the Powervision kit (Immunologic) and 3-amino-9-ethylcarbazole (AEC, Sigma-Aldrich, Zwijndrecht, the Netherlands) as a chromogen. Next, CD34 and GFAP antibodies were removed by incubating the sections at 121°C in 0.01 M citrate buffer (pH 6.0) for 10 minutes. Sections were then incubated for 1 hour at room temperature with the second primary antibody (P-gp, IgG1, JSB-1, 1:40; Abcam, or BCRP, IgG2a, BXP-21, 1:100; Abcam) and stained with a polymer-alkaline phosphatase (AP)-labeled antimouse antibody (Immunologic) and Vector Blue (AP Substrate Kit III, #SK-5300, Vector Labs, Burlingame, CA) as a chromogen. For spectral analysis (Supplementary Data Figs. S4 and S5), images were analyzed with a Nuance VIS-FL Multi-spectral Imaging System (Cambridge Research Instrumentation, Woburn, MA), as described previously (27, 28).

In addition to spectral analysis as described in the previous paragraph, double-labeling of P-gp (IgG1, JSB-1, 1:40; Abcam) or BCRP (IgG2a, BXP-21, 1:100; Abcam) with GFAP (polyclonal rabbit, DAKO, Glostrup, Denmark; 1:4000) was performed using immunofluorescence (Supplementary Data Fig. S6). Sections were incubated overnight at 4°C with primary antibodies, followed by incubation with secondary antibody Alexa Fluor 568-conjugated antirabbit and Alexa Fluor-conjugated 488 antimouse IgG (1:100, Thermo Fisher Scientific, Landsmeer, the Netherlands) for 2 hours at room temperature. Sections were then analyzed using a laser scanning confocal microscope (Leica TCS Sp2, Amsterdam, the Netherlands).

Evaluation of Immunostaining

All labeled tissue sections were evaluated for the presence or absence of various histopathological parameters and specific immunoreactivity (IR) for the different markers. P-gp

and BCRP IR was evaluated in microvessels (with size below 100 μm) and glial cells in both SC and motor cortex. The intensity of P-gp and BCRP-immunoreactive staining was evaluated using a scale of 0–3 (0: no; 1: weak; 2: moderate; 3: strong IR). See [Supplementary Data Figure S3](#) for typical examples of staining in blood vessels. The approximate proportion of cells showing IR [(i) single to 10%; (ii) 11%–50%; (iii) >50%] was also scored to give information about the relative number of positive cells within the ALS specimens. As previously reported (26), the product of these 2 values (intensity and relative number scores) gave the total score (IR score).

Western Blot

Tissue samples of the motor cortex and SC (control $n=6$, sporadic [sALS] $n=6$, and familial [fALS], $n=5$) were homogenized in lysis buffer (20 mM TRIS-HCl [pH 8], 137 mM NaCl, 1 mM Na_3VO_4 , 8% glycerol, 1% triton X-100, 2 mM EDTA, 1 mM phenylmethylsulfonyl fluoride, 10 $\mu\text{g}/\text{mL}$ leupeptin, 10 $\mu\text{g}/\text{mL}$ aprotinin, 10 $\mu\text{g}/\text{mL}$ tyrosin inhibitor). Next, they were centrifuged for 15 minutes at 18000g. Protein content was determined using the Bio-Rad (Hercules, CA) DC protein assay kit. Per sample, 40 μg of proteins was loaded on a NuPAGE 4%–12% Bis-Tris Midi protein gels, 26-well (Thermo Fisher Scientific, Waltham, MA) and electrophoreses was performed for 2 hours at 30 mA. The temperature of the running buffer (MOPS buffer [Invitrogen, Carlsbad, CA] 1:20) was maintained below 10°C. Gels were dry-blotted on nitrocellulose and these were probed for P-gp with MDR1/ABC11(E1Y7S) rabbit mAb #13978 1:1000 (Cell Signaling Technologies, Leiden, the Netherlands) or for BCRP with BXP-53 1:400 (ab24115; Abcam). Secondary HRP-antirabbit or HRP antirat 1:2000 (both from DAKO, Santa Clara, CA), respectively, were used and the blot exposed to ECL reagent (35 $\mu\text{g}/\text{mL}$ coumaric acid, 220 $\mu\text{g}/\text{mL}$ luminol, 0.0075% H_2O_2 in 100 mM TRIS pH 8.5) and images were taken on a Chemidoc XRS+ (Bio-Rad) and analyzed using Image Lab software (v5.2.1).

Statistical Analysis

Statistical analyses were performed using the GraphPad Prism software (GraphPad software Inc., La Jolla, CA). Data were analyzed with the nonparametric Kruskal-Wallis test, followed by a Dunn's post hoc test to assess the difference between groups. A p value < .05 was considered to indicate a significant difference.

RESULTS

Case Material

The clinical and neuropathological characteristics of the subjects are summarized in [Table 1](#). The cohort included 17 sALS and 8 fALS patients, patients with rapid disease progression and short-term survival (<18 months; ALS-st; $n=6$) and patients with slow disease progression and long-term survival >40 months (ALS-lt; $n=7$). Six patients (5 fALS, 1 sALS) were positive for the C9ORF72 hexanucleotide repeat

expansion. Mutations in FUS (fused in sarcoma/translocated in liposarcoma) were detected in 3 patients. There were no significant differences between the ALS and normal control groups with respect to postmortem interval or duration of tissue storage. None of the control patients had confounding neurological or neuropathological abnormalities.

P-gp and BCRP Cellular Distribution in ALS SC and Motor Cortex

[Figure 1](#) shows P-gp protein expression in a representative normal and ALS cervical SC white matter (WM) lateral corticospinal tract) and ventral horn (VH). P-gp expression was observed in endothelial cells lining the blood vessels in both control and ALS specimens ([Fig. 1](#); quantification see [Fig. 3A](#)). In controls, P-gp could not be detected in the large majority of glial cells with resting morphology ([Figs. 1A and 3B](#)). In all ALS cases, P-gp IR was evident in cells with typical glial morphology ([Figs. 1E–G and 3B](#)). A similar cellular distribution was observed in the MCx with strong expression of P-gp in blood vessels in both controls and ALS cases and higher expression in reactive astrocytes in both gray and white matter ([Figs. 2 and 3C, D](#)). Double labeling demonstrated P-gp expression in endothelial cells (CD34-positive cells; [Figs. 1H–I and 2I, Supplementary Data Fig. S4A](#) [spectral analysis]) and reactive astrocytes (GFAP-positive cells; [Figs. 1F, G and 2H, Supplementary Data Fig. S4B](#) [spectral analysis] and [Supplementary Data Fig. S6A](#) [fluorescent double labeling]), but not in cells of the microglial/macrophage lineage (HLA-DR-positive cells; [Figs. 1J and 2J](#)). In cerebellum, P-gp expression was observed in blood vessels, but could not be detected in the majority of glial cells ([Supplementary Data Fig. S1A, B](#)).

[Figure 4](#) shows BCRP protein expression in a representative normal and ALS cervical SC (VH and WM; [Fig. 4A–D](#)) and the MCx ([Fig. 4E–J](#)). BCRP expression was mainly observed in endothelial cells lining the blood vessels in both control and ALS specimens ([Fig. 4](#)). Expression of BCRP in blood vessels did not differ between control and ALS in both the both VH and WM; a modest increase of the IR score was detected for BCRP in the MCx of ALS patients ([Fig. 5E](#)). Resting glial cells did not express detectable levels of BCRP; occasionally in ALS reactive astrocytes showed BCRP expression ([Figs. 4G and 5B, D](#)). BCRP expression in blood vessels was also detected in cerebellum of both controls and ALS. ([Supplementary Data Fig. S1C, D](#)). Double labeling demonstrated BCRP expression in endothelial cells (CD34-positive cells; [Fig. 4J and Supplementary Data Fig. S5A](#)) and reactive astrocytes (GFAP-positive cells; [Fig. 4I and Supplementary Data Fig. S5B](#) [spectral analysis] and [Supplementary Data Fig. S6B](#) [fluorescent double labeling]), but not in cells of the microglial/macrophage lineage (not shown).

P-gp and BCRP glial and blood vessel IR differed neither between sALS and fALS cases in both the SC and MCx nor between patients with and without C9ORF72 hexanucleotide repeat expansion. P-gp glial expression was markedly higher compared with controls in ALS-lt, although not significantly different compared with patients with ALS-st ([Supplementary Data Fig. S2](#)).

TABLE 1. Clinical Data of Cases

Patients	Clinical Diagnosis	Gender	Site of Onset	Age (Years)	Disease Duration (Months)	C9orf72 Repeat Expansion	FUS mutation
1	sALS	M	Bulbar	75	28	–	–
2	sALS	F	Spinal ¹	61	27	–	–
3	sALS	M	Spinal ¹	60	12	–	–
4	sALS	F	Spinal ¹	61	12	–	–
5	sALS	F	Spinal ²	56	16	–	–
6	sALS	M	Spinal ²	75	19	–	–
7	sALS	F	Bulbar	65	52	–	–
8	sALS	M	Spinal ¹	50	56	–	–
9	sALS	F	Bulbar	61	43	–	–
10	sALS	M	Spinal ²	59	45	FUS	–
11	sALS	F	Spinal ²	65	25	–	–
12	sALS	M	Bulbar	53	31	C9orf72	–
13	sALS	F	Spinal ¹	56	7	–	–
14	sALS	F	Bulbar	35	20	FUS	–
15	sALS	F	Arm	70	24	FUS	–
16	sALS	F	Arm	39	130	–	–
17	sALS	M	Bulbar	58	14	–	–
18	fALS	F	Bulbar	37	26	–	–
19	fALS	M	Spinal ²	52	43	–	–
20	fALS	F	Spinal ²	64	57	C9orf72	–
21	fALS	M	Spinal ²	68	33	C9orf72	–
22	fALS	M	Spinal ²	51	23	C9orf72	–
23	fALS	F	Spinal ¹	41	16	–	–
24	fALS	M	Spinal ¹	61	33	C9orf72	–
25	fALS	F	Bulbar	66	34	C9orf72	–
1	Control	M	n/a	54	n/a	n/a	n/a
2	Control	M	n/a	56	n/a	n/a	n/a
3	Control	F	n/a	66	n/a	n/a	n/a
4	Control	F	n/a	73	n/a	n/a	n/a
5	Control	F	n/a	63	n/a	n/a	n/a
6	Control	M	n/a	65	n/a	n/a	n/a
7	Control	M	n/a	49	n/a	n/a	n/a
8	Control	F	n/a	44	n/a	n/a	n/a
9	Control	M	n/a	75	n/a	n/a	n/a
10	Control	M	n/a	48	n/a	n/a	n/a
11	Control	F	n/a	66	n/a	n/a	n/a
12	Control	F	n/a	45	n/a	n/a	n/a
13	Control	M	n/a	47	n/a	n/a	n/a
14	Control	M	n/a	63	n/a	n/a	n/a

Site of onset (region in which first symptoms occurred): Bulbar onset, spinal onset (upper 1, lower 2). Age: years. Disease duration: time from diagnosis until death in months. The ALS patients included in the study did not receive medications such as riluzole or edaravone that are substrates of P-gp and/or BCRP. Fused in sarcoma/translocated in liposarcoma (FUS), chromosome 9 open reading frame 72 (C9orf72). sALS cases without C9ORF72 hexanucleotide repeat expansion or mutations were analyzed by targeted NGS analysis. The NGS panel consists of TARBP, ALS2, ErbB4, NEK1, MATR3, VCP, SIGMAR1, c9orf72, c19orf12, OPTN, HNRNPA1, DAO, SPG11, FUS, GRN, PNPLA6, SOD1, CHCHD10, NEFH, and UBQLN2.

ALS, amyotrophic lateral sclerosis; sALS, sporadic ALS; fALS, familial ALS; M, male; F, female, n/a, not applicable.

Western blot analysis did not show differences in P-gp and BCRP expression in the motor cortex and SC between control, fALS and sALS (data not shown).

DISCUSSION

In this study, we used immunohistochemistry to compare and semiquantitatively assess ABC transporter expression at the BBB and in brain parenchyma in postmortem brain

and SC tissues of 25 ALS patients versus 11 controls. We demonstrate that P-gp expression in endothelial cells at the BBB is maintained, while a significant and strongly increased P-gp expression is observed in reactive astroglial cells in both gray (VH) and white matter of the SC, as well as in the MCx of all ALS patients, but not in cerebellum. BCRP expression was moderately but significantly increased in glia and blood vessels in the MCx of ALS patients. P-gp or BCRP IR did not

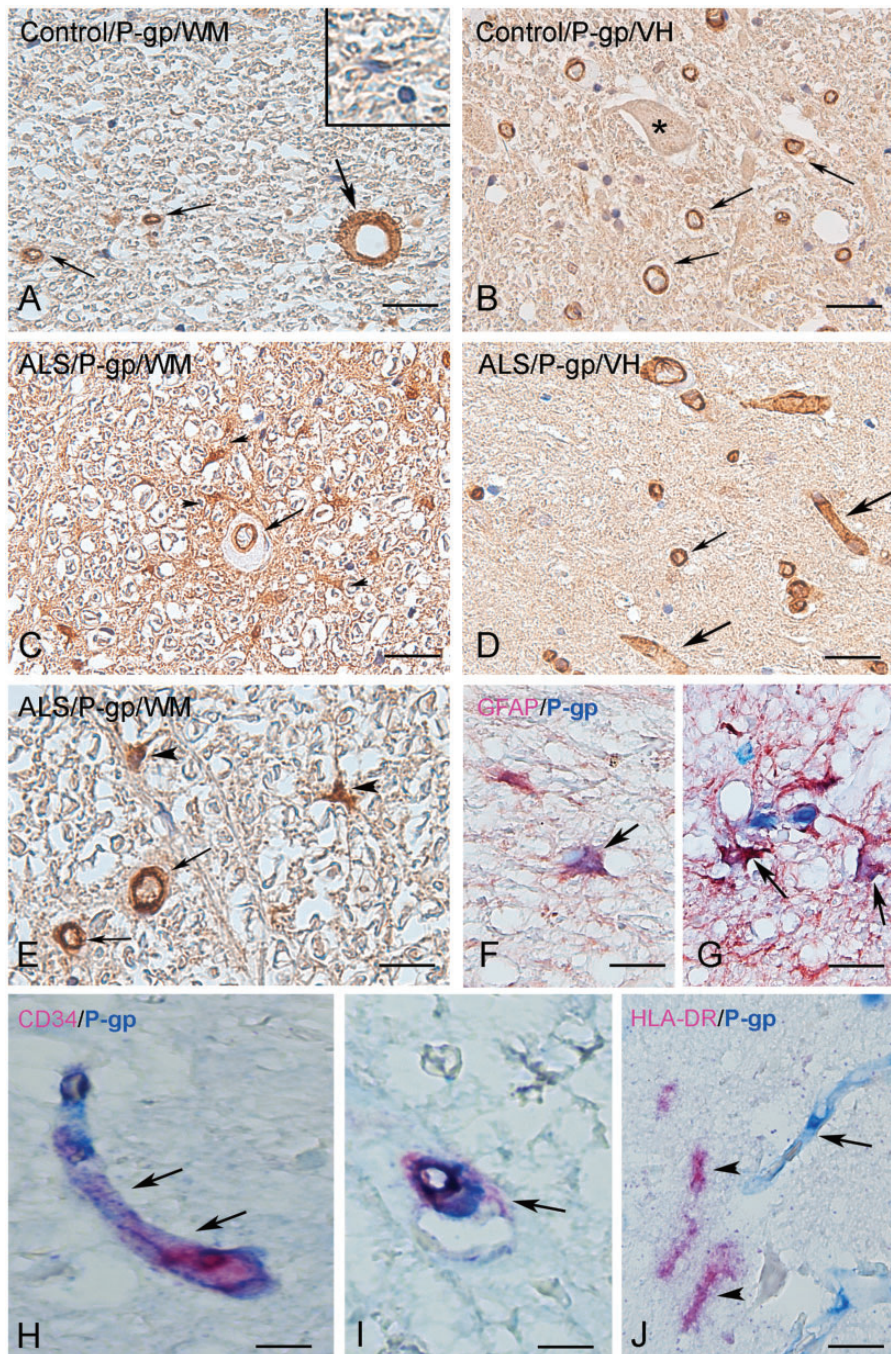


FIGURE 1. P-gp immunoreactivity in control and ALS spinal cord. **(A, B)** Representative photomicrographs of immunohistochemical staining for P-gp in control spinal cord (SC) (white matter [WM], lateral corticospinal tract; **A**; ventral horn [VH]; **B**; asterisk: negative motoneuron) showing expression in blood vessels (arrows), but no detectable immunoreactivity in the majority of glial cells (inset in **A**). **(C–G)** Representative photomicrographs of immunohistochemical staining for P-gp in ALS SC. In ALS SC immunoreactivity was observed in blood vessels (arrows in **C–E**) and reactive astrocytes in (arrowheads in **C, E**). **(F, G)** Colocalization (purple; arrows) of GFAP (red) and P-gp (blue) in reactive astrocytes (surrounding P-gp-positive vessels in **G**). **(H, I)** Colocalization (purple; arrows) of CD34 (red) and P-gp (blue) in blood vessels. **(J)** Absence of expression of P-gp (blue; arrow indicates a positive blood vessel) in cells of the microglial/macrophage lineage (arrows indicate HLA-DR-positive cells; red). Scale bars: **A–D** = 40 μm; **E, G** = 25 μm; **F, H–J** = 15 μm.

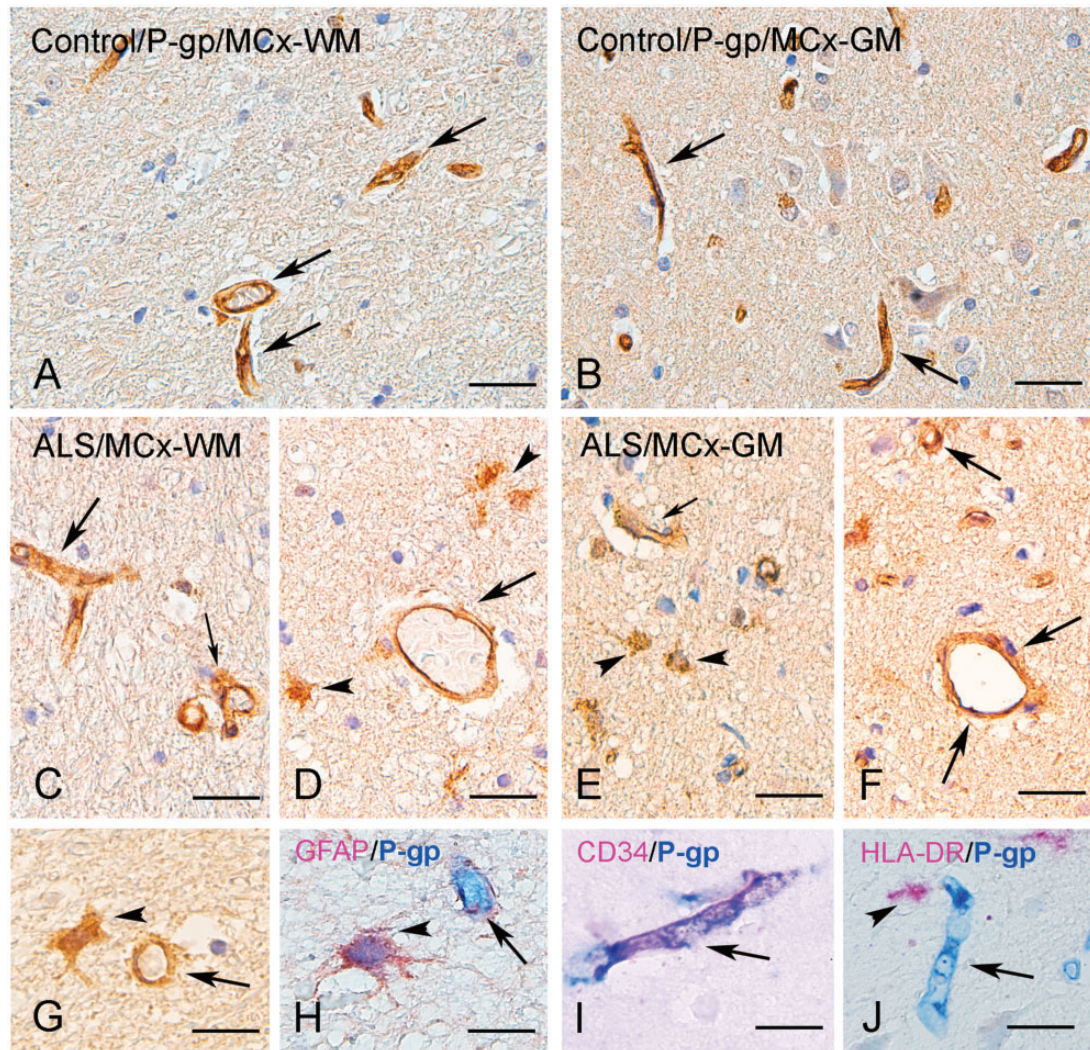


FIGURE 2. P-gp immunoreactivity in control and ALS motor cortex. **(A–C)** Representative photomicrographs of immunohistochemical staining for P-gp in control motor cortex (MCx; **A**, white matter [WM]; **B**, gray matter [GM]) showing expression in blood vessels (arrows), but in the majority of glial cells P-gp could not be detected. **(C–G)** Representative photomicrographs of immunohistochemical staining for P-gp in ALS MCx. P-gp immunoreactivity was detected in blood vessels (arrows). A substantial increase in immunoreactivity was observed in ALS motor cortex with numerous glial cells (arrowheads in **D**, **E**, **G**). **(H)** Colocalization (purple; arrow) of GFAP (red) and P-gp (blue) in reactive astrocytes (surrounding a P-gp-positive vessel). **(I)** Colocalization (purple; arrow) of CD34 (red) and P-gp (blue) in a blood vessel. **(J)** Absence of expression of P-gp (blue; arrow indicates a positive blood vessel) in cells of the microglial/macrophage lineage (arrow indicate an HLA-DR-positive cell; red). Scale bars: **A–F** = 40 μ m; **G–J** = 15 μ m.

differ between sALS and fALS cases. This higher expression is in line with results from a previous study in a small set of patients (12). In contrast to the immunohistochemical findings, we could not detect differences in P-gp or BCRP expression between groups using Western blot analysis. This can most likely be explained by the fact that tissue homogenates are used for Western blot, which is not particularly suitable to discern relatively small differences in expression at the cellular level.

BBB impairment is an early event in the pathogenesis of patients with ALS (15) as in other neurodegenerative diseases (29, 30). Also, in the SOD1 mouse model for ALS, increased

permeability of the BBB was an early symptom that occurred prior to motor neuron loss (31). Perturbation of tight junctions increases the leakiness of the BBB as shown in ALS (31) and other neurodegenerative disorders (32–35). While entry of potentially neurotoxic macromolecules such as hemoglobin and albumin through a more permeable BBB may be an underlying cause of ALS, a higher permeability could potentially facilitate the entry of therapeutics into diseased CNS tissues. On the other hand, however, upregulation of the drug efflux pumps P-gp and BCRP, as seen in this study in ALS patients and in patients with HIV encephalitis (36), multiple sclerosis (37) and glioblastoma (31), may result in an attenuation of the

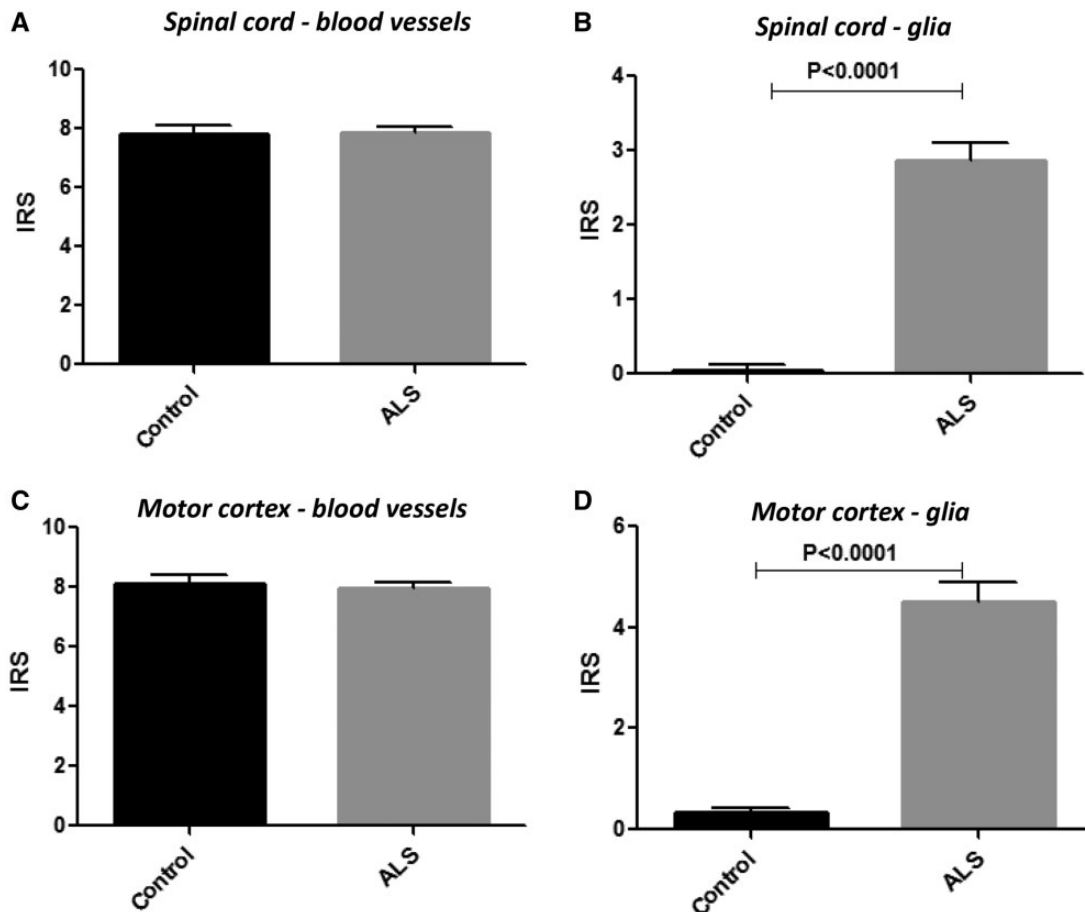


FIGURE 3. P-gp immunoreactivity scores in control and ALS spinal cord and motor cortex. Plots showing P-gp mean immunoreactivity score (IRS) in blood vessels (microvessels, size $<100\ \mu\text{m}$) and glial cells (astrocytes) in control ($n = 14$) and ALS cases ($n = 25$). The IRS represents the mean total score, which was taken as the product of the intensity score and the relative number score (for details see Materials and Methods section).

efficacy of therapeutics. In SOD1-G93A and TDP-43 rodent models, disease progression correlated with a selective upregulation of P-gp and BCRP, both at the mRNA and protein level, in homogenized SC tissues (12, 19, 24, 38). Concomitant administration of the dual P-gp/BCRP inhibitor elacridar improved the efficacy of riluzole in SOD1-G93A ALS mice, indicating that pharmaco-resistance is at least partially mediated by drug efflux transporters (12, 21).

P-gp (encoded by ABCB1) and BCRP (encoded by ABCG2) unidirectional efflux pumps are widely distributed in the body, with high expression at the BBB, the intestines, liver and in stem cells (39, 40). BCRP and P-gp have broad and overlapping substrate specificities, including many known drugs, and they function redundantly or synergistically in removing substrate drugs from pump-protected cells and tissues, causing multidrug resistance (40–46). Comparisons of wild-type versus ABC-transporter knockout mice demonstrate that absence of both P-gp and BCRP caused a redistribution of substrate drugs from peripheral tissues into pump-protected “sanctuary tissues,” such as the brain without affecting plasma levels (40, 41, 46–49).

Clinical studies in ALS patients demonstrated that riluzole is effective and even showed disease-modifying activity in early stage, but this benefit was transient and lost in late stage (50). In 155 ALS patients, mortality was reduced by 38% during the first 12 months of treatment and this benefit was reduced to 19% at 21 months (51). Edaravone, which is the only other approved drug for treatment of ALS, also demonstrated efficacy (i.e. reduced functional decline or ALSFRS-R score) but also only in a subset of patients with early stage ALS (52). Several other agents that demonstrated benefit in preclinical models failed to show efficacy in clinical trials (53) (Table 2). Although lack of efficacy may have various roots, this may include suboptimal drug exposure due to insufficient BBB penetration. In fact, approximately 98% of all FDA-approved small molecule drugs do not maintain effective exposure in the brain often also due to the action of P-gp and/or BCRP (54–56). Consequently, adequate penetration of the BBB by any novel candidate therapeutic remains an important consideration when testing a novel therapy. Dual inhibitors of P-gp and BCRP, such as elacridar, may help to improve therapy (12, 21). Moreover, in our study we observed an increased expression,

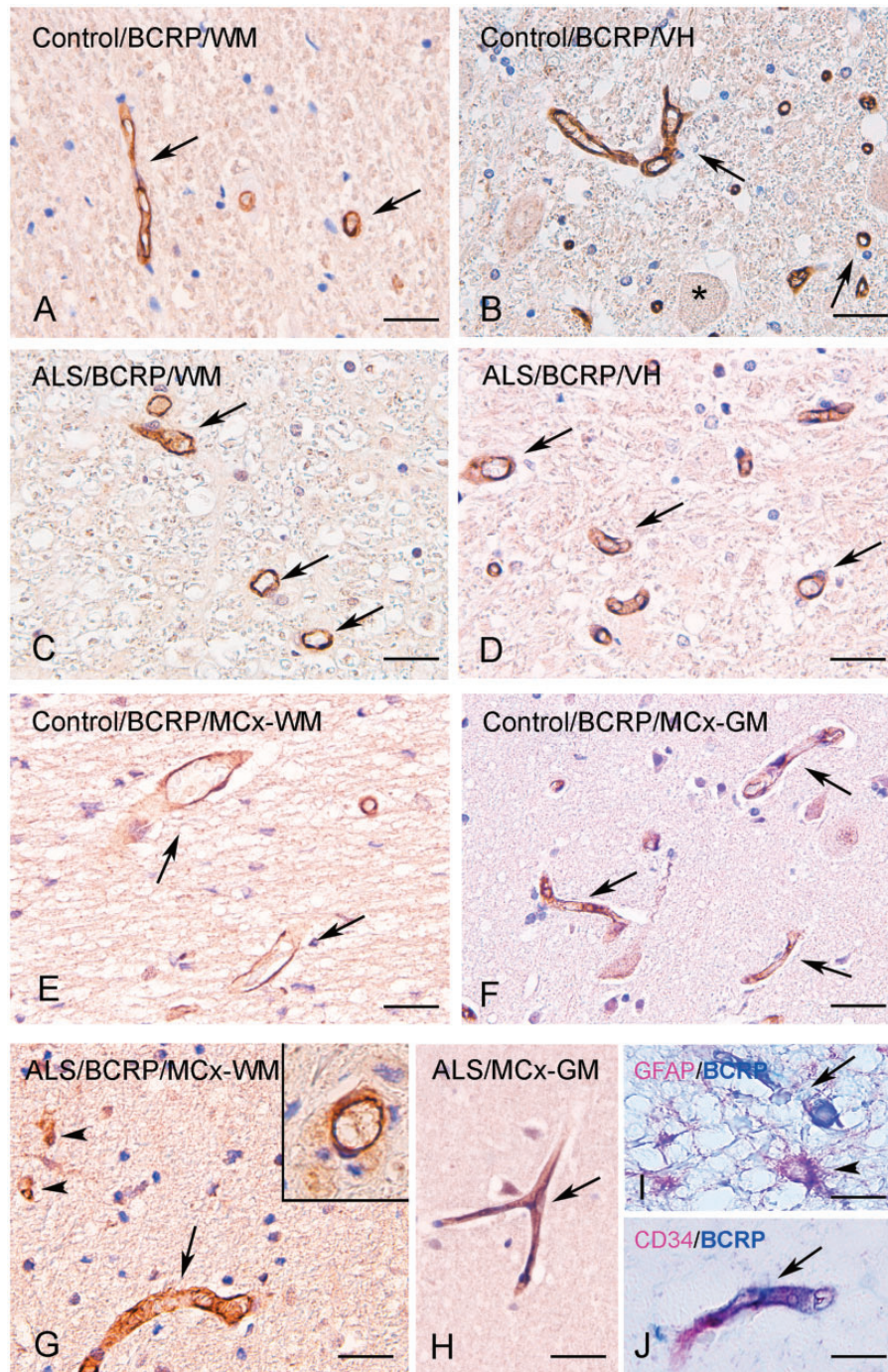


FIGURE 4. BCRP immunoreactivity in control and ALS spinal cord and motor cortex. **(A, B)** Representative photomicrographs of immunohistochemical staining for BCRP in control spinal cord (SC) (white matter [WM], lateral corticospinal tract; **A**; ventral horn, **B**; asterisk shows a negative motoneuron), showing expression in blood vessels (arrows). **(C, D)** Representative photomicrographs of immunohistochemical staining for BCRP in ALS SC showing expression in blood vessels (arrows). **(E, F)** Representative photomicrographs of immunohistochemical staining for BCRP in control motor cortex (MCx; **E**, WM; **F**, gray matter, [GM]) showing weak to moderate expression in blood vessels (arrows). **(G, H)** Representative photomicrographs of immunohistochemical staining for BCRP in ALS motor cortex. BCRP immunoreactivity was detected in blood vessels (arrows); occasionally a few positive glial cells were observed (arrowheads in **G**; around a positive blood vessel, inset in **G**). **(I)** Colocalization (purple; arrowhead) of GFAP (red) and BCRP (blue) in reactive astrocytes (surrounding a BCRP-positive vessel). **(J)** Colocalization (purple; arrow) of CD34 (red) and BCRP (blue) in a blood vessel. Scale bars: **A–H** = 40 μ m; **G–J** = 20 μ m.

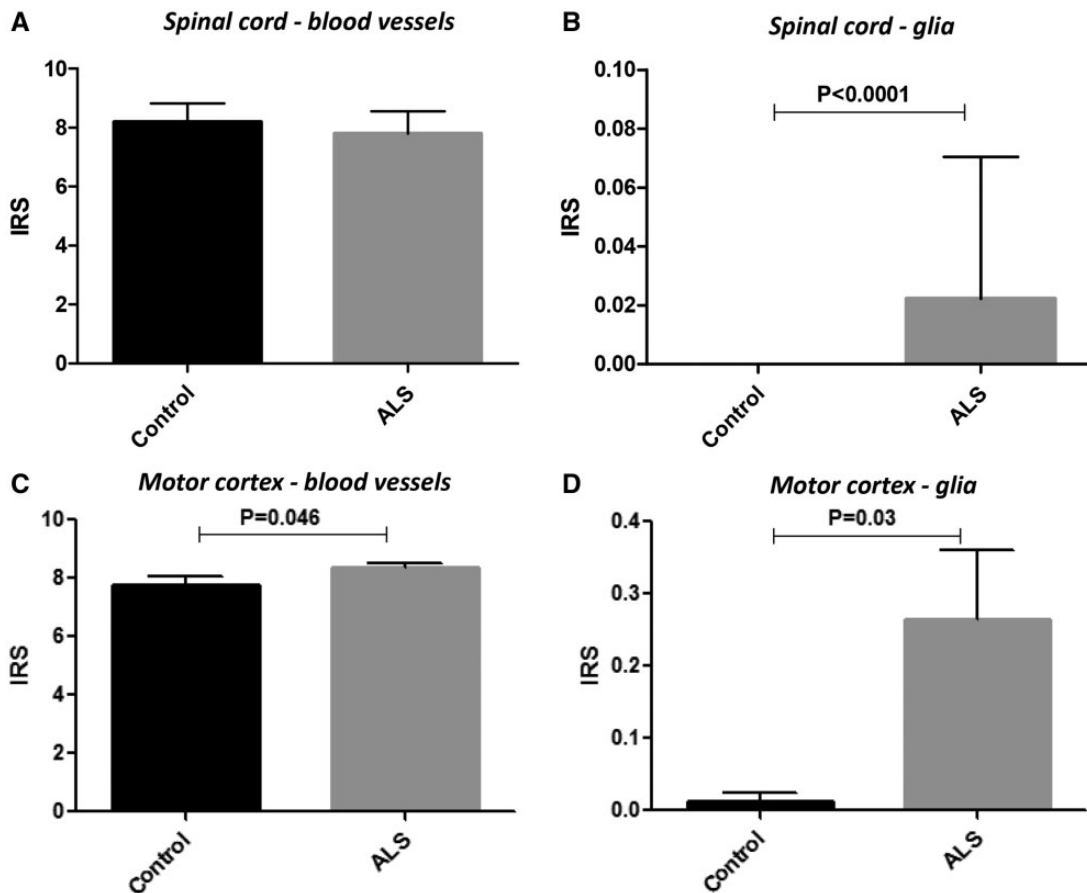


FIGURE 5. BCRP immunoreactivity scores in control and ALS spinal cord and motor cortex. Plots showing BCRP mean immunoreactivity score (IRS) in blood vessels (microvessels, size <100 μm) and glial cells (astrocytes) in control (n = 14) and ALS (n = 25) cases. The IRS represents the mean total score, which was taken as the product of the intensity score and the relative number score (see Materials and Methods section for details).

TABLE 2. FDA-Approved Drugs With Strong Preclinical Data, Failed in ALS Clinical Trials

ALS status	Drug	References P-gp/BCRP Substrate
FDA approved	Riluzole	(20, 21, 61, 62)
	Edaravone IV	(63)
Not approved	Masitinib	(64)
	Cyclosporin	(65, 66)
	Ceftriaxone	(67)
	Celecoxib	(68, 69)
	(Dex)pramipexole	(70)
	Gabapentin	(71, 72)
	Minocycline	(20)
	rHCNTF	(73)
	Topiramate	(72, 74)
	Vitamin E	(75, 76)
Candidate	Raltegravir	(44, 77)
	Imatinib	(78)

particularly of P-gp in astrocytes within the affected brain regions in both sALS and fALS cases. Accordingly, increased expression of ABC-transporters in perivascular and parenchymal astrocytes has also been reported in various pharmacoresistant neurological disorders (18). Astrocytes represent a key component of the neurovascular unit and several studies highlight the role of astrocytes in maintaining P-gp expression in BBB-endothelial cells, thereby restricting the penetration of xenobiotics into the CNS (57). Interestingly, apart from removal of xenobiotics, P-gp in astrocytes may act as modulator of the immune response regulating the secretion of inflammatory molecules (36, 58), and several studies indicate a complex regulation of their astroglial expression by pro-inflammatory pathways (18). Recently, it has also been shown that astrocytes harboring ALS causative mutations (i.e. FUS and SOD1m, but not C9orf72) drive P-gp upregulation in endothelial cells through soluble factors, including inflammatory molecules, as well as glutamate (14, 59).

In conclusion, our results show high expression of P-gp and BCRP at the blood-brain and SC barrier in healthy

controls and ALS patients. In addition, in ALS patients we observed a strong upregulation of P-gp in astrocytes in both the SC and MCx, whereas BCRP showed a moderate increase in glial cells and blood vessels in cortex. The ALS patients included in the study did not receive medications such as riluzole or edaravone that are substrates of P-gp and/or BCRP. However, the use of drugs which induce ABC-transporters could represent a contributing factor leading to the ABC-transporter-mediated multidrug resistance in ALS patients (60). The high expression of both drug efflux pumps may thwart the efficacy of approved substrate drugs (riluzole, edaravone) and obstruct the successful employment of other novel candidate agents. ALS is a debilitating and deadly disease with very few therapeutic options. Besides the obvious need of identifying appropriate targets and targeted therapeutics for better therapy, this ABC-transporter-mediated multidrug resistance calls for effective strategies to ensure adequate BBB-crossing and therapeutic drug exposure.

ACKNOWLEDGMENTS

We acknowledge the team who helped in the collection of ALS tissue samples (Prof. Dr. D. Troost, Prof. Dr. M. de Visser, Dr. A.J. van der Kooij, and Dr. J. Raaphorst).

REFERENCES

- Kiernan MC, Vucic S, Cheah BC, et al. Amyotrophic lateral sclerosis. *Lancet* 2011;377:942–55
- Saberi S, Stauffer JE, Schulte DJ, et al. Neuropathology of amyotrophic lateral sclerosis and its variants. *Neurol Clin* 2015;33:855–76
- Strong MJ. Revisiting the concept of amyotrophic lateral sclerosis as a multisystemic disorder of limited phenotypic expression. *Curr Opin Neurol* 2017;30:599–607
- Morris HR, Waite AJ, Williams NM, et al. Recent advances in the genetics of the ALS-FTLD complex. *Curr Neurol Neurosci Rep* 2012;12:243–50
- Lee SE, Sias AC, Mandelli ML, et al. Network degeneration and dysfunction in presymptomatic C9ORF72 expansion carriers. *Neuroimage Clin* 2017;14:286–97
- Al-Chalabi A, van den Berg LH, Veldink J. Gene discovery in amyotrophic lateral sclerosis: Implications for clinical management. *Nat Rev Neurol* 2017;13:96–104
- Blokhuis AM, Groen EJ, Koppers M, et al. Protein aggregation in amyotrophic lateral sclerosis. *Acta Neuropathol* 2013;125:777–94
- Edens BM, Miller N, Ma YC. Impaired autophagy and defective mitochondrial function: Converging paths on the road to motor neuron degeneration. *Front Cell Neurosci* 2016;10:44
- Riancho J, Gonzalo I, Ruiz-Soto M, et al. Why do motor neurons degenerate? Actualization in the pathogenesis of amyotrophic lateral sclerosis. *Neurologia* 2019;34:27–37
- Gordon PH. Amyotrophic lateral sclerosis: Pathophysiology, diagnosis and management. *CNS Drugs* 2011;25:1–15
- Lee J, Ryu H, Keum G, et al. Therapeutic targeting of epigenetic components in amyotrophic lateral sclerosis (ALS). *CMC* 2014;21:3576–82
- Jablonski MR, Jacob DA, Campos C, et al. Selective increase of two ABC drug efflux transporters at the blood-spinal cord barrier suggests induced pharmacoresistance in ALS. *Neurobiol Dis* 2012;47:194–200
- Jablonski M, Miller DS, Pasinelli P, et al. ABC transporter-driven pharmacoresistance in Amyotrophic Lateral Sclerosis. *Brain Res* 2015;1607:1–14
- Mohamed LA, Markandaiah S, Bonanno S, et al. Blood-brain barrier driven pharmacoresistance in amyotrophic lateral sclerosis and challenges for effective drug therapies. *AAPS J* 2017;19:1600–14
- Garbuzova-Davis S, Sanberg PR. Blood-CNS Barrier Impairment in ALS patients versus an animal model. *Front Cell Neurosci* 2014;8:21
- Mizuno N, Niwa T, Yotsumoto Y, et al. Impact of drug transporter studies on drug discovery and development. *Pharmacol Rev* 2003;55:425–61
- Loscher W, Potschka H. Blood-brain barrier active efflux transporters: ATP-binding cassette gene family. *Neurotherapeutics* 2005;2:86–98
- Aronica E, Sisodiya SM, Gorter JA. Cerebral expression of drug transporters in epilepsy. *Adv Drug Deliv Rev* 2012;64:919–29
- Boston-Howes W, Williams EO, Bogush A, et al. Nordihydroguaiaretic acid increases glutamate uptake in vitro and in vivo: Therapeutic implications for amyotrophic lateral sclerosis. *Exp Neurol* 2008;213:229–37
- Milane A, Fernandez C, Dupuis L, et al. P-glycoprotein expression and function are increased in an animal model of amyotrophic lateral sclerosis. *Neurosci Lett* 2010;472:166–70
- Jablonski MR, Markandaiah SS, Jacob D, et al. Inhibiting drug efflux transporters improves efficacy of ALS therapeutics. *Ann Clin Transl Neurol* 2014;1:996–1005
- Qosa H, Miller DS, Pasinelli P, et al. Regulation of ABC efflux transporters at blood-brain barrier in health and neurological disorders. *Brain Res* 2015;1628:298–316
- Qosa H, Lichter J, Sarlo M, et al. Astrocytes drive upregulation of the multidrug resistance transporter ABCB1 (P-Glycoprotein) in endothelial cells of the blood-brain barrier in mutant superoxide dismutase 1-linked amyotrophic lateral sclerosis. *Glia* 2016;64:1298–313
- Chan GN, Evans RA, Banks DB, et al. Selective induction of P-glycoprotein at the CNS barriers during symptomatic stage of an ALS animal model. *Neurosci Lett* 2017;639:103–13
- Ludolph A, Drory V, Hardiman O, et al. A revision of the El Escorial criteria – 2015. *Amyotroph Lateral Scler Frontotemporal Degener* 2015;16:291–2
- Casula M, Iyer AM, Spliet WG, et al. Toll-like receptor signaling in amyotrophic lateral sclerosis spinal cord tissue. *Neuroscience* 2011;179:233–43
- van der Loos CM. Multiple immunoenzyme staining: Methods and visualizations for the observation with spectral imaging. *J Histochem Cytochem* 2008;56:313–28
- Boer K, Troost D, Timmermans W, et al. Cellular localization of metabotropic glutamate receptors in cortical tubers and subependymal giant cell tumors of tuberous sclerosis complex. *Neuroscience* 2008;156:203–15
- Abbott NJ, Ronnback L, Hansson E. Astrocyte-endothelial interactions at the blood-brain barrier. *Nat Rev Neurosci* 2006;7:41–53
- Obermeier B, Daneman R, Ransohoff RM. Development, maintenance and disruption of the blood-brain barrier. *Nat Med* 2013;19:1584–96
- Wijaya J, Fukuda Y, Schuetz JD. Obstacles to brain tumor therapy: Key ABC transporters. *Int J Mol Sci* 2017;18.
- Lewandowski SA, Fredriksson L, Lawrence DA, et al. Pharmacological targeting of the PDGF-CC signaling pathway for blood-brain barrier restoration in neurological disorders. *Pharmacol Ther* 2016;167:108–19
- Stanimirovic DB, Friedman A. Pathophysiology of the neurovascular unit: Disease cause or consequence? *J Cereb Blood Flow Metab* 2012;32:1207–21
- Zlokovic BV. The blood-brain barrier in health and chronic neurodegenerative disorders. *Neuron* 2008;57:178–201
- Bartels AL, Willemsen AT, Kortekaas R, et al. Decreased blood-brain barrier P-glycoprotein function in the progression of Parkinson's disease, PSP and MSA. *J Neural Transm* 2008;115:1001–9
- Langford D, Grigorian A, Hurford R, et al. Altered P-glycoprotein expression in AIDS patients with HIV encephalitis. *J Neuropathol Exp Neurol* 2004;63:1038–47
- Kooij G, Mizee MR, van Horssen J, et al. Adenosine triphosphate-binding cassette transporters mediate chemokine (C-C motif) ligand 2 secretion from reactive astrocytes: Relevance to multiple sclerosis pathogenesis. *Brain* 2011;134:555–70
- Wegorzewska I, Bell S, Cairns NJ, et al. TDP-43 mutant transgenic mice develop features of ALS and frontotemporal lobar degeneration. *Proc Natl Acad Sci U S A* 2009;106:18809–14
- Szakacs G, Paterson JK, Ludwig JA, et al. Targeting multidrug resistance in cancer. *Nat Rev Drug Discov* 2006;5:219–34
- Robey RW, Pluchino KM, Hall MD, et al. Revisiting the role of ABC transporters in multidrug-resistant cancer. *Nat Rev Cancer* 2018;18:452–64
- Neul C, Schaeffeler E, Sparreboom A, et al. Impact of membrane drug transporters on resistance to small-molecule tyrosine kinase inhibitors. *Trends Pharmacol Sci* 2016;37:904–32
- Loscher W, Potschka H. Drug resistance in brain diseases and the role of drug efflux transporters. *Nat Rev Neurosci* 2005;6:591–602

43. Lin T, Islam O, Heese K. ABC transporters, neural stem cells and neurogenesis—A different perspective. *Cell Res* 2006;16:857–71
44. Weiss J, Haefeli WE. Impact of ATP-binding cassette transporters on human immunodeficiency virus therapy. *Int Rev Cell Mol Biol* 2010;280:219–79
45. Eyal S, Hsiao P, Unadkat JD. Drug interactions at the blood-brain barrier: Fact or fantasy? *Pharmacol Ther* 2009;123:80–104
46. Agarwal S, Hartz AM, Elmquist WF, et al. Breast cancer resistance protein and P-glycoprotein in brain cancer: Two gatekeepers team up. *CPD* 2011;17:2793–802
47. Kim RB, Fromm MF, Wandel C, et al. The drug transporter P-glycoprotein limits oral absorption and brain entry of HIV-1 protease inhibitors. *J Clin Invest* 1998;101:289–94
48. Wang JS, Ruan Y, Taylor RM, et al. The brain entry of risperidone and 9-hydroxyrisperidone is greatly limited by P-glycoprotein. *Int J Neuropharmacol* 2004;7:415–9
49. de Vries NA, Buckle T, Zhao J, et al. Restricted brain penetration of the tyrosine kinase inhibitor erlotinib due to the drug transporters P-gp and BCRP. *Invest New Drugs* 2012;30:443–9
50. Zoccolella S, Beghi E, Palagano G, et al. Riluzole and amyotrophic lateral sclerosis survival: A population-based study in southern Italy. *Eur J Neurol* 2007;14:262–8
51. Bensimon G, Lacomblez L, Meininger V. A controlled trial of riluzole in amyotrophic lateral sclerosis. ALS/Riluzole Study Group. *N Engl J Med* 1994;330:585–91
52. Abe K, Aoki M, Tsuji S, et al. Safety and efficacy of edaravone in well defined patients with amyotrophic lateral sclerosis: A randomised, double-blind, placebo-controlled trial. *Lancet Neurol* 2017;16:505–12
53. Petrov D, Mansfield C, Moussy A, et al. ALS clinical trials review: 20 years of failure. Are we any closer to registering a new treatment? *Front Aging Neurosci* 2017;9:68
54. Pardridge WM. Blood-brain barrier delivery. *Drug Discov Today* 2007;12:54–61
55. Hitchcock SA. Blood-brain barrier permeability considerations for CNS-targeted compound library design. *Curr Opin Chem Biol* 2008;12:318–23
56. Weiss N, Miller F, Cazaubon S, et al. The blood-brain barrier in brain homeostasis and neurological diseases. *Biochim Biophys Acta* 2009;1788:842–57
57. Lecuyer MA, Kebir H, Prat A. Glial influences on BBB functions and molecular players in immune cell trafficking. *Biochim Biophys Acta* 2016;1862:472–82
58. Kooij G, Backer R, Koning JJ, et al. P-glycoprotein acts as an immunomodulator during neuroinflammation. *PLoS One* 2009;4:e8212
59. Mohamed LA, Markandaiah SS, Bonanno S, et al. Excess glutamate secreted from astrocytes drives upregulation of P-glycoprotein in endothelial cells in amyotrophic lateral sclerosis. *Exp Neurol* 2019;316:27–38
60. Calcagno AM, Kim IW, Wu CP, et al. ABC drug transporters as molecular targets for the prevention of multidrug resistance and drug-drug interactions. *CDD* 2007;4:324–33
61. Milane A, Vautier S, Chacun H, et al. Interactions between riluzole and ABCG2/BCRP transporter. *Neurosci Lett* 2009;452:12–6
62. Dulin JN, Moore ML, Grill RJ. The dual cyclooxygenase/5-lipoxygenase inhibitor licofelone attenuates p-glycoprotein-mediated drug resistance in the injured spinal cord. *J Neurotrauma* 2013;30:211–26
63. Parikh A, Kathawala K, Tan CC, et al. Self-nanomicellizing solid dispersion of edaravone: Part I – Oral bioavailability improvement. *DDDT* 2018;12:2051–69
64. Kocic I, Kowianski P, Rusiecka I, et al. Neuroprotective effect of masitinib in rats with postischemic stroke. *Naunyn-Schmiedeberg's Arch Pharmacol* 2015;388:79–86
65. Schinkel AH, Wagenaar E, van Deemter L, et al. Absence of the mdr1a P-Glycoprotein in mice affects tissue distribution and pharmacokinetics of dexamethasone, digoxin, and cyclosporin A. *J Clin Invest* 1995;96:1698–705
66. Kirkinetzos IG, Hernandez D, Bradley WG, et al. An ALS mouse model with a permeable blood-brain barrier benefits from systemic cyclosporine A treatment. *J Neurochem* 2004;88:821–6
67. Kato Y, Takahara S, Kato S, et al. Involvement of multidrug resistance-associated protein 2 (Abcc2) in molecular weight-dependent biliary excretion of beta-lactam antibiotics. *Drug Metab Dispos* 2008;36:1088–96
68. Rahman M, Selvarajan K, Hasan MR, et al. Inhibition of COX-2 in colon cancer modulates tumor growth and MDR-1 expression to enhance tumor regression in therapy-refractory cancers in vivo. *Neoplasia* 2012;14:624–33
69. Zhang XQ, Zhang HM, Sun XE, et al. Inhibitory effects and mechanism of 5-fluorouracil combined with celecoxib on human gastric cancer xenografts in nude mice. *Exp Ther Med* 2015;9:105–11
70. Vautier S, Milane A, Fernandez C, et al. Interactions between antiparkinsonian drugs and ABCB1/P-glycoprotein at the blood-brain barrier in a rat brain endothelial cell model. *Neurosci Lett* 2008;442:19–23
71. West CL, Mealey KL. Assessment of antiepileptic drugs as substrates for canine P-glycoprotein. *Am J Vet Res* 2007;68:1106–10
72. Nakanishi H, Yonezawa A, Matsubara K, et al. Impact of P-glycoprotein and breast cancer resistance protein on the brain distribution of antiepileptic drugs in knockout mouse models. *Eur J Pharmacol* 2013;710:20–8
73. Monville C, Fages C, Feyens AM, et al. Astroglial expression of the P-glycoprotein is controlled by intracellular CNTF. *BMC Cell Biol* 2002;3:20
74. Sills GJ, Kwan P, Butler E, et al. P-glycoprotein-mediated efflux of anti-epileptic drugs: Preliminary studies in mdr1a knockout mice. *Epilepsy Behav* 2002;3:427–32
75. Mustacich DJ, Vo AT, Elias VD, et al. Regulatory mechanisms to control tissue alpha-tocopherol. *Free Radic Biol Med* 2007;43:610–8
76. Traber MG, Labut EM, Leonard SW, et al. alpha-Tocopherol injections in rats up-regulate hepatic ABC transporters, but not cytochrome P450 enzymes. *Free Radic Biol Med* 2011;51:2031–40
77. Kis O, Robillard K, Chan GN, et al. The complexities of antiretroviral drug-drug interactions: Role of ABC and SLC transporters. *Trends Pharmacol Sci* 2010;31:22–35
78. Oostendorp RL, Buckle T, Beijnen JH, et al. The effect of P-gp (Mdr1a/1b), BCRP (Bcrp1) and P-gp/BCRP inhibitors on the in vivo absorption, distribution, metabolism and excretion of imatinib. *Invest New Drugs* 2009;27:31–40